Lin *et al. Virology Journal* (2024) 21:245
https://doi.org/10.1186/s12985-024-02502-y

Virology Journal

RESEARCH Open Access

Oncolytic activity of a coxsackievirus B3 strain in patient-derived cervical squamous cell carcinoma organoids and synergistic effect with paclitaxel

Yanzhen Lin[1†], Nanyi Liu[2,3†], Chuanlai Yang[2,3], Haoyin Tan[2,3], Changjian Fang[2,3], Kang Yu[2,3], Huan Zhao[2,3], Ningshao Xia[2,3], Wei Wang[2,3*], Xiumin Huang[1*] and Tong Cheng[2,3*]

Abstract

Background Cervical squamous cell carcinoma (CSCC) is a prevalent gynecological malignancy worldwide. Current treatments for CSCC can impact fertility and cause long-term complications, underscoring the need for new therapeutic strategies. Oncolytic virotherapy has emerged as a promising option for cancer treatment. Previous research has demonstrated the oncolytic activity of the coxsackievirus B3 strain 2035 A (CVB3/2035A) against various tumor types. This study aims to evaluate the clinical viability of CVB3/2035A for CSCC treatment, focusing on its oncolytic effect in patient-derived CSCC organoids.

Methods The oncolytic effects of CVB3/2035A were investigated using human CSCC cell lines in vitro and mouse xenograft models in vivo. Preliminary tests for tumor-selectivity were conducted on patient-derived CSCC tissue samples and compared to normal cervical tissues ex vivo. Three patient-derived CSCC organoid lines were developed and treated with CVB3/2035A alone and in combination with paclitaxel. Both cytotoxicity and virus replication were evaluated in vitro.

Results CVB3/2035A exhibited significant cytotoxic effects in human CSCC cell lines and xenograft mouse models. The virus selectively induced oncolysis in patient-derived CSCC tissue samples while sparing normal cervical tissues ex vivo. In patient-derived CSCC organoids, which retained the immunohistological characteristics of the original tumors, CVB3/2035A also demonstrated significant cytotoxic effects and efficient replication, as evidenced by increased viral titers and presence of viral nucleic acids and proteins. Notably, the combination of CVB3/2035A and paclitaxel resulted in enhanced cytotoxicity and viral replication.

†Yanzhen Lin and Nanyi Liu have contributed equally to this work.

*Correspondence:
Wei Wang
lukewang@xmu.edu.cn
Xiumin Huang
huangxmxm@163.com
Tong Cheng
tcheng@xmu.edu.cn

Full list of author information is available at the end of the article

Conclusions CVB3/2035A showed oncolytic activity in CSCC cell lines, xenografts, and patient-derived tissue cultures and organoids. Furthermore, the virus exhibited synergistic anti-tumor effects with paclitaxel against CSCC. These results suggest CVB3/2035A could serve as an alternative or adjunct to current CSCC chemotherapy regimens.

Keywords Coxsackievirus B3, Cervical squamous cell carcinoma, Organoid, Oncolytic virus, Virotherapy

Introduction

Cervical cancer is the fourth most common malignancy among women worldwide, with approximately 600,000 new cases and over 300,000 deaths reported annually [1]. Cervical squamous cell carcinoma (CSCC), the predominant histological subtype of cervical cancer, accounts for 70% of all cases and originates from the stratified squamous epithelium of the ectocervix. Most CSCCs are associated with sexually transmitted high-risk HPV infections, particularly HPV16 and HPV18 [2]. Current treatment options include surgery, radiation, chemotherapy, immunotherapy, or a combination of these approaches. Although the disease generally shows a favorable prognosis post-treatment, the chosen methods can impact fertility or lead to a high incidence of long-term sequelae [3]. Therefore, there is a pressing need to develop new therapeutic approaches to treat CSCC.

Oncolytic viruses (OVs) are emerging as promising candidates for cancer therapy due to their ability to selectively replicate within tumor cells and effectively destroy them while sparing normal cells [4]. Currently, four OV products have been approved for marketing, with numerous others in development [5]. Coxsackievirus B3 (CVB3), a small, non-enveloped enterovirus with a single-stranded, positive-sense RNA genome in the *Picornaviridae* family, has shown significant oncolytic potential. The prototype Nancy strain of CVB3 (CVB3/Nancy) has demonstrated oncolytic activity against a wide range of human tumor cell lines [6]. In addition, another CVB3 strain, 2035 A (CVB3/2035A), exhibits oncolytic activity against various cancer types, including colon, stomach, lung, liver, ovarian, endometrial, and cervical cancers [7]. CVB3 preferentially replicates in and lyses actively proliferating tumor cells rather than normal cells, since oncogenic signaling pathways and impaired type I interferon signaling in tumor cells create a favorable microenvironment for viral replication [4]. Moreover, the virus's entry receptor, the coxsackievirus and adenovirus receptor (CAR), is highly expressed in various cancer types [8]. These characteristics suggest that CVB3 strains may serve as promising oncolytic agents for cancer therapy, including CSCC.

In the realm of CSCC preclinical modeling, cell lines and cell line-derived xenografts (CDXs) are the most commonly used tools [9]. Moreover, patient-derived tumor xenografts (PDXs), which maintain key features from their parental tumors such as genetic and phenotypic heterogeneity, have become important preclinical models [10]. However, PDXs have low generation efficiency and are not suitable for large-scale drug screening [11]. Recently, CSCC organoids derived from tumor stem cells have been developed. These organoids preserve the essential features of the original tumors and can be established and expanded with high efficiency. This in vitro model provides a platform for various basic research activities, including high-throughput drug sensitivity screening [12]. Patient-derived CSCC organoids have been utilized to assess the response to chemotherapeutic agents, with several studies demonstrating a positive correlation between the drug response of tumor organoids and patients [2, 13–16]. In this study, CSCC cell lines and patient-derived CSCC organoids were used to evaluate the potential clinical benefits of oncolytic CVB3/2035A alone and in combination with the standard chemotherapeutic agent paclitaxel (PTX) for treating CSCC. The findings indicate that CVB3/2035A holds promise as a candidate for CSCC virotherapy.

Methods

Cells and virus

Three human CSCC cell lines (C33A, SiHa, and CaSki) were purchased from the American Type Culture Collection (ATCC). All cells were maintained in 5% CO_2 at 37 ℃ in Dulbecco's modified Eagle's medium (DMEM) supplemented with 10% fetal bovine serum (FBS) and 1% penicillin-streptomycin solution (All from Thermo Fisher Scientific).

CVB3/2035A strain (GenBank Accession No. KY286529.1) was isolated in 2008 from a throat swab of a patient with mild hand, foot and mouth disease at the Centers for Disease Control and Prevention in Xiamen, China. The virus was then propagated in Hela cells (ATCC). Virus titers were determined in Hela cells using the $TCID_{50}$ assay according to the Reed-Muench method.

In vitro viral infectivity assay

C33A, SiHa, or CaSki cells were seeded in 96-well plates in DMEM without FBS and then infected with 10-fold serial dilutions of CVB3/2035A (50 µL/well in quadruplicate, from MOI=10 to MOI=0.01). After incubation in 5% CO_2 at 37 ℃ for 72 h, cytotoxicity was assessed using a Cell Counting Kit-8 (CCK-8) assay according to the manufacturer's instructions (MCE, HY-K0301).

Flow cytometry analysis

C33A, SiHa, or CaSki cells were incubated with rabbit polyclonal antibodies against CAR (Abcam, ab100811), followed by incubation with fluorescein isothiocyanate (FITC)-conjugated goat anti-rabbit secondary antibodies (Sigma, AP132F). The cells were then washed, centrifuged, resuspended in PBS, and analyzed for receptor expression using a flow cytometer (BD Bioscience, BD FACSAria™ III). The data were analyzed using FlowJo software version 10.8.1.

In vivo anti-tumor studies using subcutaneous xenografts in nude mice

All animal procedures were conducted under specific pathogen-free (SPF) conditions and in accordance with the approved animal use protocols of Xiamen University Laboratory Animal Center. For xenografts in BALB/c nude mice, 5×10^6 cells (C33A, SiHa, and CaSki) were subcutaneously injected into the right flanks of 6-8-week-old female BALB/c nude mice (GemPharmatech, China). When tumors reached diameters of approximately 6 mm, the mice were inoculated with CVB3/2035A and/or PTX. To evaluate the effectiveness of CVB3/2035A, mice received intratumoral (i.t.) or intravenous (i.v.) injections of five consecutive doses (1×10^8 $TCID_{50}$ per dose) of CVB3/2035A at two-day intervals. The same volume of PBS was administered i.t. as a negative control. To evaluate the combined effect of CVB3/2035A and PTX, mice were either mock-treated or received i.t. injections of CVB3/2035A (1×10^8 $TCID_{50}$), intraperitoneal (i.p.) injections of PTX (5 mg/kg [17]; diluted in solution containing 10% DMSO, 40% PEG300, 5% Tween-80, and 45% saline [18]), or a combination administered five times consecutively at two-day intervals. Tumor sizes were measured with calipers every other day for 20 days. The tumor volume was calculated as length×width×width/2 and expressed as means ± SEM.

Sample collection

Seven human CSCC tissue samples were collected from patients at Zhongshan Hospital of Xiamen University during surgical resection procedures (Table S1). Three normal cervical tissues were obtained from patients who underwent a hysterectomy performed for benign uterine diseases. None of the CSCC patients received any treatment before surgery. We utilized four CSCC tissue samples and three normal cervical tissues for the histoculture drug response assay, while the remaining three CSCC tissue samples were employed for organoid derivation. Informed consent for this study was obtained from each patient. This study received approval from both the hospital's Institutional Review Board and the Research Ethics Committee of Xiamen University. Experiments were carried out in strict accordance with the guidelines and regulations of Xiamen University.

Histoculture drug response assay

Four CSCC tissue samples and three normal cervical tissues were used in the histoculture drug response assay (HDRA) with slight modifications to a previous protocol [19]. Briefly, collagen gel sponges were cut into 1 cm cubes and placed in the wells of a 24-well plate, followed by the addition of 1 mL DMEM medium containing 20% FBS and 10% penicillin/streptomycin solution. The tissues were minced into approximately 1-mm diameter pieces and randomly placed on the collagen gel sponges in the 24-well plate. After an overnight culture at 37 ℃, the tissues were either exposed to 1×10^7 $TCID_{50}$ of CVB3/2035A per well or left untreated. Following a 72-hour incubation, 100 µL of 0.06% collagenase (type IV; Sigma) in DMEM was added to each well, and the plates were incubated at 37 ℃ for another 4 h. Subsequently, the tissues and supernatants from each well were harvested and centrifuged at 5,000 g for 10 min (mins) at 4 ℃. The resultant pellets from each well were resuspended in 100 µL DMEM medium, and cell viability was assessed using the CCK-8 assay in 96-well plates. The inhibition rate was calculated using the following formula: Inhibition rate (%) = (1 − A/B) × 100, where A represents the mean absorbance of the treated wells per 1 g of tumor, and B represents the mean absorbance of the control wells per 1 g of tumor.

Quantitative RT-PCR (qRT-PCR)

RNA was extracted from tissue homogenates using a GenMagSpin Viral DNA/RNA Kit (GenMag Bio, China). Real-time PCR analysis was performed with the primers (forward, 5'-TCCTCCGGCCCCTGA-3'; reverse, 5'-AAT TGTCACCATAAGCAGCCA-3'; and probe, 5'-FAM-CG GAACCGACTACTTTGGGTGTCCGT-BHQ1-3') using a One-Step RT-PCR Kit (GenMag Bio, China) and Roche 96 system according to the manufacturer's protocol. The thermal conditions were set to 50 ℃ for 10 min, 95 ℃ for 10 min, followed by 45 cycles of 95 ℃ for 15 s (secs) and 55 ℃ for 50 s. Relative cDNA level was calculated using a standard curve of Ct (cycle threshold) values generated from the dilution series of pMD18-CVB3/2035A plasmid containing the target gene.

Immunohistochemistry assay

The expression of CAR in four CSCC tumors and three normal tissues used in HDRA was assessed by immunohistochemistry (IHC). Tumor sections (5 µm) underwent heat-induced antigen retrieval using citrate buffer, followed by endogenous peroxidase quenching using hydrogen peroxide. The sections were then incubated with rabbit anti-CAR antibodies (Abcam, ab100811) for

one hour at room temperature. Subsequently, IHC staining was performed using an Ultrasensitive TMS-P kit (Fuzhou Maixin Biotechnology Development Co., Ltd., China) and a DAB detection kit (streptavidin-biotin; Fuzhou Maixin Biotechnology Development Co., Ltd., China) according to the manufacturer's instructions. Finally, the sections were counterstained with hematoxylin, dehydrated, and cover-slipped. CAR staining was quantified using ImageJ (version 1.0) and presented as relative optical density normalized to sections incubated with PBS.

Establishment and culture of CSCC organoids

Three CSCC tissue samples were washed and disinfected in DPBS containing 10% penicillin/streptomycin for 5 min. Subsequently, the tissues were sectioned into small pieces, with some used for immunofluorescence analysis and the remainder for organoid derivation. A tissue dissociation solution was prepared by mixing 10 mL of AdDF+++ (Advanced DMEM/F12 supplemented with 1×Glutamax, 10 mM HEPES, and penicillin-streptomycin, all from Thermo Fisher Scientific), 10 μM RHO/ROCK pathway inhibitor (TargetMol, Y-27632), and 1 mg/mL type I and type IV collagenase (Gibco, 17100017; Gibco, 17104019). The tissue samples intended for organoid derivation were finely chopped in this dissociation solution and then dissociated on an orbital shaker at 37 °C for one hour. Following centrifugation, trypsin digestion was performed for 30 min. Upon completion of the digestion process, the sample was filtered through a 70 μm cell strainer. After an additional round of centrifugation, red blood cells were removed from the sample using a red blood cell lysis buffer (Solarbio, R1010). Then, 10 mL of AdDF+++ was added, and the suspension was centrifuged at 500 g for 3 min.

The cell pellets were resuspended in cold basement membrane extract (BME; R&D Systems, 3536-005-02). Next, 120 μL drops of the BME cell suspension were allowed to solidify on pre-warmed 6-well culture plates at 37 °C for 30 min. Following this, organoid growth medium [AdDF+++ supplemented with 100 ng/mL Noggin (R&D Systems, 6057-NG-100), 500ng/mL RSPO1 (R&D Systems, 4645-RS-250), 1× B27 supplement (GIBCO, 175044), 2.5 mM nicotinamide (Sigma, N0636), 1.25 mM n-Acetylcystein (Sigma, A9165), 10 μM ROCK inhibitor (TargetMol, Y-27632), 500 nM A83-01 (Tocris, 2939), 10 μM forskolin (Bio-Techne, 1099), 25 ng/ml FGF7 (SinoBiological, 10210-H07E), 100 ng/ml FGF10 (SinoBiological, 10573-HNAE), and 1 μM p38 inhibitor SB202190 (Sigma, S7067)] was prepared as previously described [2] and 4 mL added to each well. The plate was placed in a 37 °C/5% CO_2 incubator and medium was refreshed every 2 to 3 days. Growth was monitored every 2 days using the Opera Phenix High-Content Screening System (PerkinElmer).

Immunofluorescence assay of CSCC organoids and original tumors

For immunofluorescence analysis of uninfected CSCC organoids and original tumors, samples cultured in CellCarrier Ultra microplates (PerkinElmer) were fixed with 4% paraformaldehyde, permeabilized with 3% Triton-X, washed with PBS, blocked with 2% BSA for one hour, and incubated overnight at 4 °C with antibodies against Ki67 (Novus Biologicals, NB110-89717), p53 (Cell Signaling Technology, 2527S), PAX8 (Cell Signaling Technology, 59019S), PanCK (Abcam, ab7753), or CAR (Abcam, ab100811). Subsequently, the samples were washed five times with PBS and incubate for one hour at 37 °C with Alexa Fluor 647-labeled goat-anti-rabbit (Beyotime, A0468) or goat-anti-mouse (Beyotime, A0473) secondary antibodies. The nuclei and cytoskeleton were counterstained with DAPI (Beyotime, C1002) and phalloidin (Thermo Fisher Scientific, A12379), respectively. Immunofluorescence data were acquired and analyzed using the Harmony® High-Content Imaging and Analysis Software (PerkinElmer, version 4.9).

For immunofluorescence analysis of CVB3/2035A-infected organoids, samples were fixed with 4% paraformaldehyde, embedded in O.C.T., sectioned into 5 μm thick frozen sections on glass slides, and dehydrated at -20 °C using a 1:1 methanol and acetone mixture. The sections were then blocked with 2% BSA for one hour, followed by overnight incubation at 4 °C with antibodies against double-stranded RNA (J2; Scicons, 10010200) and CVB3/2035A VP1 (clone L8F12, produced in our lab, unpublished). After rinsing five times with PBS, the sections were incubated with Alexa Fluor 647-labeled goat-anti-mouse secondary antibody (Beyotime, A0473) at room temperature for one hour and subsequently stained with DAPI (Beyotime, C1002). Immunofluorescence imaging was performed using the Leica LAS X Widefield Systems Fluorescence Microscope System.

Infection of CSCC organoids and viral growth kinetics

Cultrex Organoid Harvesting Solution (50 μL Solution /5 μL BME; R&D Systems) was added to the organoids, followed by incubation at 4°C for 60 min to digest the BME. The organoids were then mechanically dissociated by pipetting and filtered through a 100 μm strainer to remove large clusters. Subsequently, the organoids were resuspended in growth medium at a concentration of 5,000 organoids/mL and plated in a volume of 100 μL on 96-well ultra-low attachment plates, according to the previous protocol [20, 21], each containing approximately 5×10^4 cells/ well counted after trypsin digestion. Serial 10-fold dilutions of CVB3/2035A, ranging from 1×10^8

to 1×10^5 $TCID_{50}$/well, were added in 25 µL volumes. The plates were incubated at 37 °C with 5% CO_2 for 72 h. For combinatorial treatment strategies, PTX was included in the medium at a final concentration of 2 µM, as reference in [22]. For the evaluation of viral growth kinetics, supernatants from the infected organoids were harvested at 4, 12, 24, and 48 h post-treatment, and virus titers were determined in Hela cells using the $TCID_{50}$ assay.

Cell viability assay of CSCC organoids

Seventy-two hours following the addition of CVB3/2035A, either alone or in combination with PTX, cellular ATP levels in the organoids were quantified using the Cell Titer-Glo 3D Cell Viability Assay (Promega), according to the manufacturer's instructions. Luminescence readings were obtained with the EnSight Multimode Plate Reader (PerkinElmer). These results were normalized against a blank control containing an equal volume of PBS, and the data were analyzed for cell viability using GraphPad Prism 9. In addition, the organoids were stained with DAPI and propidium iodide (PI) to visualize the nuclei and dead cells. Fluorescence imaging was subsequently carried out using the Opera Phenix High-Content Screening System (PerkinElmer) to analyze cell viability.

Statistical analysis

All statistical analyses were performed using GraphPad Prism 9. We used Student's *t*-test, one-way ANOVA, two-way ANOVA, and Tukey's multiple comparisons test for statistical significance. The significance levels were denoted as follows: $^{*}p<0.05$; $^{**}p<0.01$; $^{***}p<0.001$; $^{****}p<0.0001$; ns, not significant.

Results

Oncolytic activity of CVB3/2035A in human CSCC cell lines and cell line-derived xenografts

To assess the oncolytic potential of CVB3/2035A against human CSCC, we first conducted in vitro studies using the CSCC cell lines C33A, SiHa, and CaSki. Cell monolayers were infected with CVB3/2035A at different MOIs (10-fold series, ranging from 10 to 0.01) and incubated at 37 °C for 72 h. Microscopic examination revealed extensive cell lysis across all three cell lines (Fig. 1A). CCK8 assays indicated that CVB3/2035A induced over 50% cytotoxicity in C33A and CaSki cells at MOIs≥0.01 and in SiHa cells at MOIs≥0.1, demonstrating potent oncolytic activity in vitro (Fig. 1B). Flow cytometry analysis showed that the oncolytic activity of CVB3/2035A correlated with the expression levels of the viral receptor CAR on the cell surface (Fig. S1A).

Secondly, the in vivo oncolytic effects of CVB3/2035A were evaluated using BALB/c nude mice bearing subcutaneous CSCC cell-derived xenografts. When the xenografts reached approximately 6 mm in diameter, the mice received five i.t. or i.v. injections of CVB3/2035A (1×10^8 $TCID_{50}$/dose) at two-day intervals. Tumor volumes were measured over a 20-day period. Both i.t. and i.v. treatments with CVB3/2035A achieved complete elimination of C33A CDX and induced significant tumor regression in SiHa and CaSki CDXs (Fig. 1C). In addition, combination therapies with CVB3/2035A and the chemotherapeutic drug PTX were explored. Mice received five consecutive i.t. treatments of 1×10^8 $TCID_{50}$ CVB3/2035A, i.p. treatments of 5 mg/kg PTX, or combination treatments at two-day intervals. The combination therapy resulted in significantly slower tumor growth in SiHa and CaSki xenografts compared to treatments with either agent alone. In the C33A xenografts, complete tumor elimination was achieved in all CVB3/2035A treatment groups, except for the group treated with PTX alone (Fig. 1D). No significant side effects or differences in body weight were observed between the treatment and control groups (Fig. S1B-C). Histopathological analysis showed no evident damage to major organs (Fig. S2). Overall, CVB3/2035A demonstrated significant oncolytic activity in human CSCC cell lines and xenografts.

Oncolytic activity of CVB3/2035A in patient-derived CSCC samples ex vivo

To assess the tumor selectivity and potential clinical efficacy of CVB3/2035A in CSCC treatment, surgical specimens from four CSCC patients (sample information shown in Table S1) and three normal cervical samples were collected to test CVB3/2035A-mediated oncolysis. Tumor or normal tissue slices (~1 mm^3) were cultured ex vivo and either infected with CVB3/2035A (1×10^7 $TCID_{50}$/well) or left untreated ($n=3$ per group). CVB3/2035A-treatment resulted in a 30–50% decrease in the viability of patient-derived CSCC tissues while causing minimal damage to normal cervical tissues (Fig. 2A). Replication of CVB3/2035A, evaluated by qRT-PCR, showed higher levels of viral RNA in patient-derived CSCC tissues compared to normal cervical tissues (Fig. 2B). The variations in cytotoxicity and viral replication may be related to differences in CAR expression between CSCC and normal cervical tissues (Fig. S3). These data preliminarily suggest that CVB3/2035A possesses tumor-selective characteristics and has potential for clinical therapeutic use against CSCC.

Establishment and characterization of CSCC organoids

Ex vivo cultured tumor tissues provide clinically relevant models for drug evaluation; however, the limited availability of clinical samples hampers high-throughput and in-depth analysis. To address this limitation, we constructed patient-derived CSCC organoid models to further evaluate the oncolytic activity of CVB3/2035A.

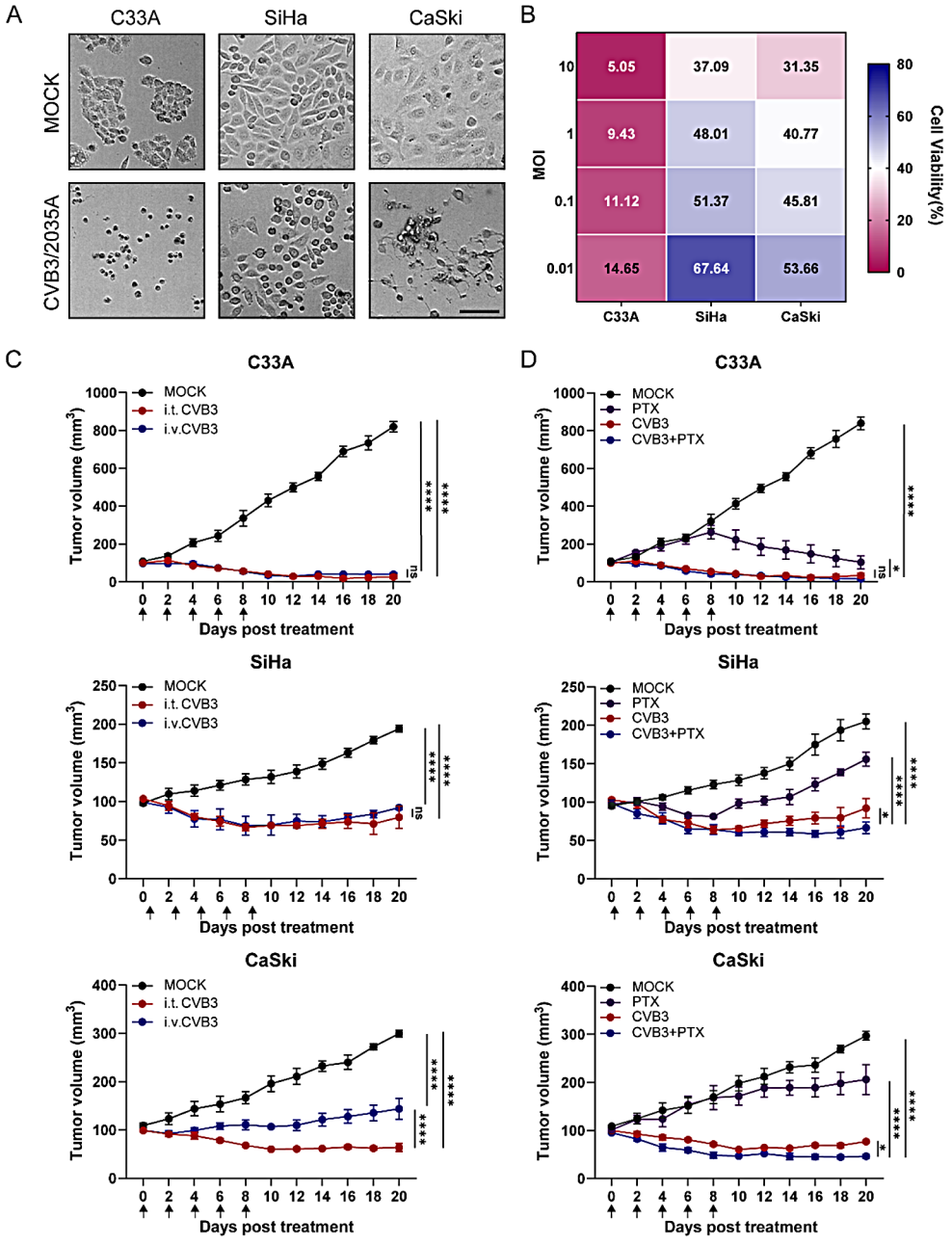

Fig. 1 Oncolytic activity of CVB3/2035A in human CSCC cell lines and cell line-derived xenografts. **(A)** CSCC cell monolayers were either mock-infected or infected with CVB3/2035A at an MOI of 1. Photomicrographs were taken at 72 h post-infection. Scale bar, 100 μm. **(B)** CSCC cells were infected with CVB3/2035A at an MOI of 10, 1, 0.1, and 0.01 for 72 h. Cell viability was assessed using the CCK8 assay. **(C)** Nude mice bearing C33A, SiHa, and CaSki xenografts were treated i.t. or i.v. with five consecutive doses of CVB3/2035A (1×10^8 $TCID_{50}$ per dose). An equivalent volume of PBS was administered i.t. as a control (Mock). Tumor growth was monitored over a 20-day period. **(D)** The combination of CVB3/2035A and paclitaxel improved efficacy in CSCC CDX models. Nude mice with C33A, SiHa, and CaSki xenografts were either mock-treated (PBS i.t. + PTX diluting solution i.p.) or treated with CVB3/2035A (1×10^8 $TCID_{50}$ i.t. + PTX diluting solution i.p.), PTX (5 mg/kg i.p. + PBS i.t.), or a combination (1×10^8 $TCID_{50}$ CVB3/2035A i.t. + 5 mg/kg PTX i.p.). Data are presented as means ± SEM. Statistical analysis was performed using a two-way ANOVA ($n=5$). Black arrows indicate treatments; ns, not significant; *$p<0.05$; ****$p<0.0001$

Tumor samples were obtained from three CSCC patients who provided consent for surgical resection. These samples were used to create organoid models and for immunohistological analysis. The tumor tissues were dissociated into single cells using collagenase and trypsin, then embedded into a basement membrane extract, seeded, and cultured in growth media to develop tumor organoids, as illustrated in Fig. 3A. Within 11 days, all three CSCC organoid lines exhibited rapid growth, forming organoids ranging from 100 to 200 μm in

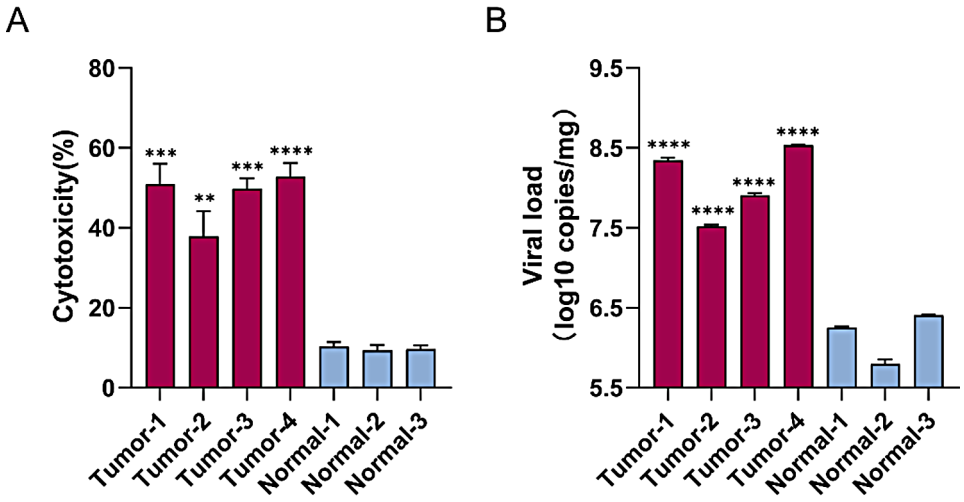

Fig. 2 Oncolytic effect of CVB3/2035A on patient-derived CSCC samples ex vivo. Four CSCC samples (Tumor 1–4) and three normal cervical samples (Normal 1–3) were divided into approximately 1-mm^3 pieces and treated with CVB3/2035A (1×10^7 $TCID_{50}$/well) or left untreated ($n=3$ per group). After 72 h, (**A**) tissue viability was assessed using a modified HDRA method, and (**B**) replication of CVB3/2035A in both tumor and normal tissue samples was quantified by qRT-PCR. Statistical analysis was performed by comparing each tumor sample's value to the mean value of all three normal samples using one-way ANOVA. Data are presented as means ± SEM. $^{**}p<0.01$; $^{***}p<0.001$; $^{****}p<0.0001$

diameter. Variability in growth rates was observed among the organoid lines (Fig. 3B-C and Fig. S4), with measurements on days 1, 7, and 11 showing significant size increases (Fig. 3C). These results demonstrate the successful establishment of three CSCC organoid lines capable of substantial growth in a short period.

Next, immunofluorescence analysis was conducted on three matched tumor-organoid pairs to evaluate the preservation of immunohistological characteristics from the original tumor samples in the CSCC organoids. The analysis revealed that the marker expression profiles of each organoid line were consistent with those of the original tumors (Fig. 3D and Fig. S5). Notably, high expression levels of the proliferation marker Ki67 and strong nuclear staining for p53 were observed. All pairs showed enriched expression for PanCK and negative expression for PAX8, confirming their epithelial nature and supporting the ectocervical origin of CSCC. Furthermore, the cellular CVB3 receptor CAR was detected in both the organoids and original tumors. The proportions of cells positive for Ki67, p53, PanCK, and CAR were quantitatively evaluated (Fig. 3E). In addition to the significantly increased proportion of PanCK-positive cells in CSCC organoid lines, other markers showed no significant differences compared to the original tumors. Moreover, we compared the proportions of CAR-positive cells among three CSCC organoid lines. Results showed that the proportions of CAR-positive cells in the CSCC-1 and CSCC-2 organoid lines were significantly higher than in the CSCC-3 organoid line ($p=0.0043$ and $p<0.0001$ respectively). These results demonstrate the immunohistological similarity between CSCC organoids and their original tumor counterparts.

Oncolytic activity of CVB3/2035A in CSCC organoids

The CSCC organoids, fragmented into small clusters, were grown in 96-well ultra-low attachment plates and infected with 10-fold serial dilutions of CVB3/2035A, ranging from 1×10^8 to 1×10^5 $TCID_{50}$/well. At 72 h post-infection (hpi), cell viability was assessed using the Cell Titer-Glo 3D assay, which revealed dose-dependent cytotoxicity induced by CVB3/2035A. Notably, >50% cytotoxicity was observed in the CSCC-1 and CSCC-2 organoid lines with an initial infection dose of $\geq1\times10^7$ $TCID_{50}$/well, and in the CSCC-3 organoid line with an initial dose of $\geq1\times10^8$ $TCID_{50}$/well (Fig. 4A). At the high dose of 1×10^8 $TCID_{50}$/well, CSCC-1 and CSCC-2 exhibited significantly higher cytotoxicity compared to CSCC-3 ($p<0.0001$ and $p=0.0001$, respectively; Fig. S6A), indicating varying sensitivity to virus-induced tumor cell lysis among the different organoid lines.

To further investigate tumor cell death, organoids treated with 1×10^7 $TCID_{50}$/well of CVB3/2035A were analyzed using brightfield microscopy and PI staining at 72 hpi (Fig. 4B). Brightfield microscopy revealed virus-induced lytic breakdown of organoids, characterized by blurred edges and abundant cellular debris. In addition, PI staining provided clearer visualization of cell death within the organoids, with positive cells predominantly localized in the outer layers, likely due to direct viral exposure. Collectively, these results, along with those from the cell viability assay, indicate that CVB3/2035A exhibits oncolytic activity in all three CSCC organoid lines in vitro.

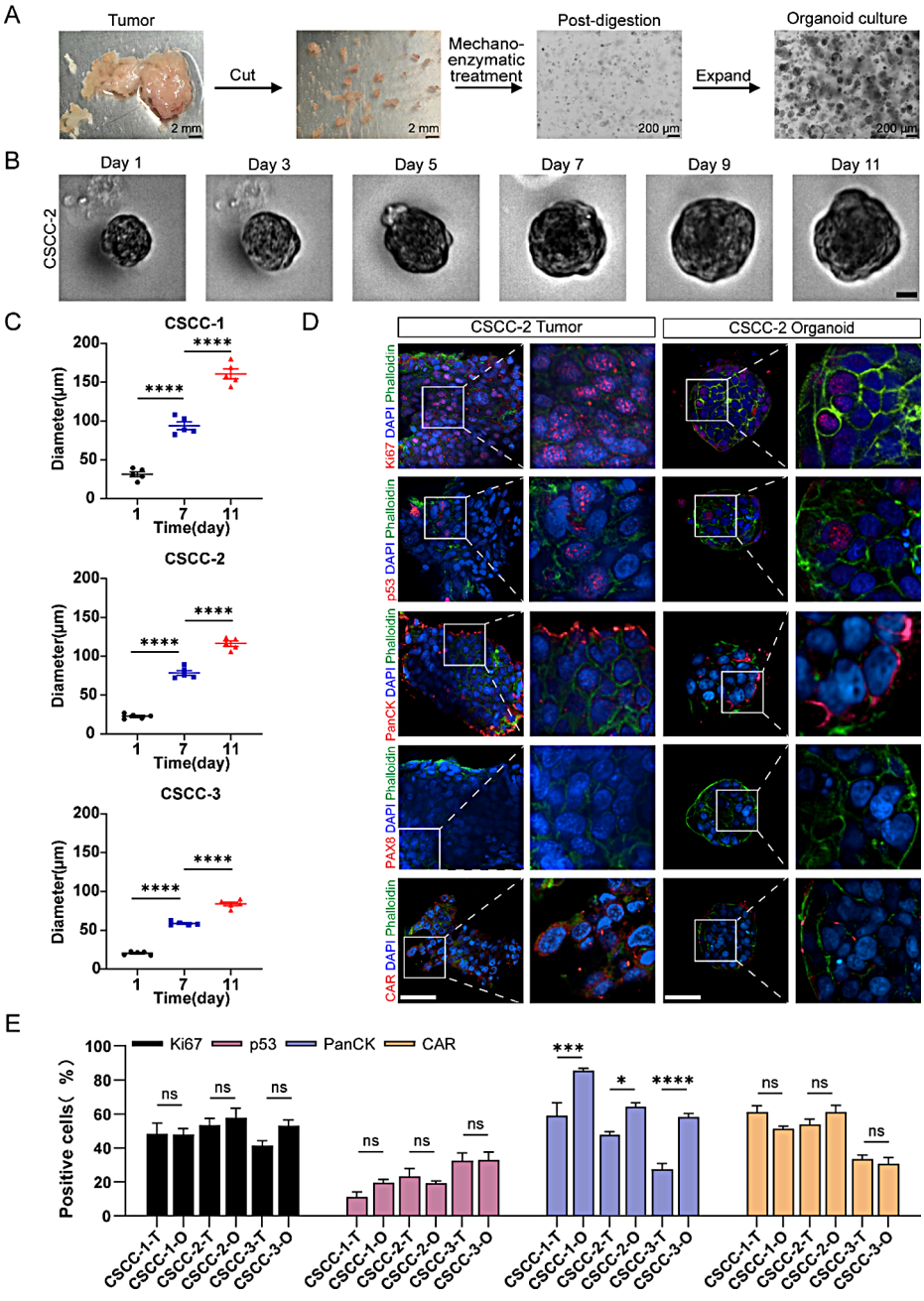

Fig. 3 Generation of CSCC Organoids. **(A)** Schematic illustration of the derivation of CSCC organoids from patient samples. **(B)** Representative brightfield microscopy images of CSCC organoids post-seeding (exemplified by CSCC-2; see Fig. S4 for more examples). Scale bar, 25 μm. **(C)** Measurements of the growth diameters of CSCC organoids at days 1, 7, and 11. Horizontal lines and error bars represent the mean diameter ± SEM for five organoids ($n = 5$). **(D)** Immunohistological features of CSCC organoids derived from patients, compared to original tumors (exemplified by CSCC-2, see Fig. S5 for more examples). Representative immunofluorescence images display markers Ki67, p53, PanCK, PAX8, and CAR (all in red), with nuclei counterstained using DAPI (blue) and cell membranes with phalloidin (green). Inset images from the left panels are magnified three-fold in the right panels for enhanced detail. Scale bar, 50 μm. **(E)** Proportion of immunofluorescence staining-positive cells in primary tumors and organoids ($n = 3$). Statistical significance was assessed using two-way ANOVA. T, tumor; O, organoid; ns, not significant; *$p < 0.05$; ***$p < 0.001$; ****$p < 0.0001$; ns, not significant

Replication of CVB3/2035A in CSCC organoids

Replication of oncolytic viruses in cancer cells can significantly increase the viral load, potentially enhancing overall oncolytic activity by infecting and impacting more nearby cancer cells. Therefore, it is crucial to examine the replication capacity of CVB3/2035A in CSCC organoids. Firstly, the organoids were infected with 10-fold serial dilutions of CVB3/2035A, ranging from 1×10^8 to

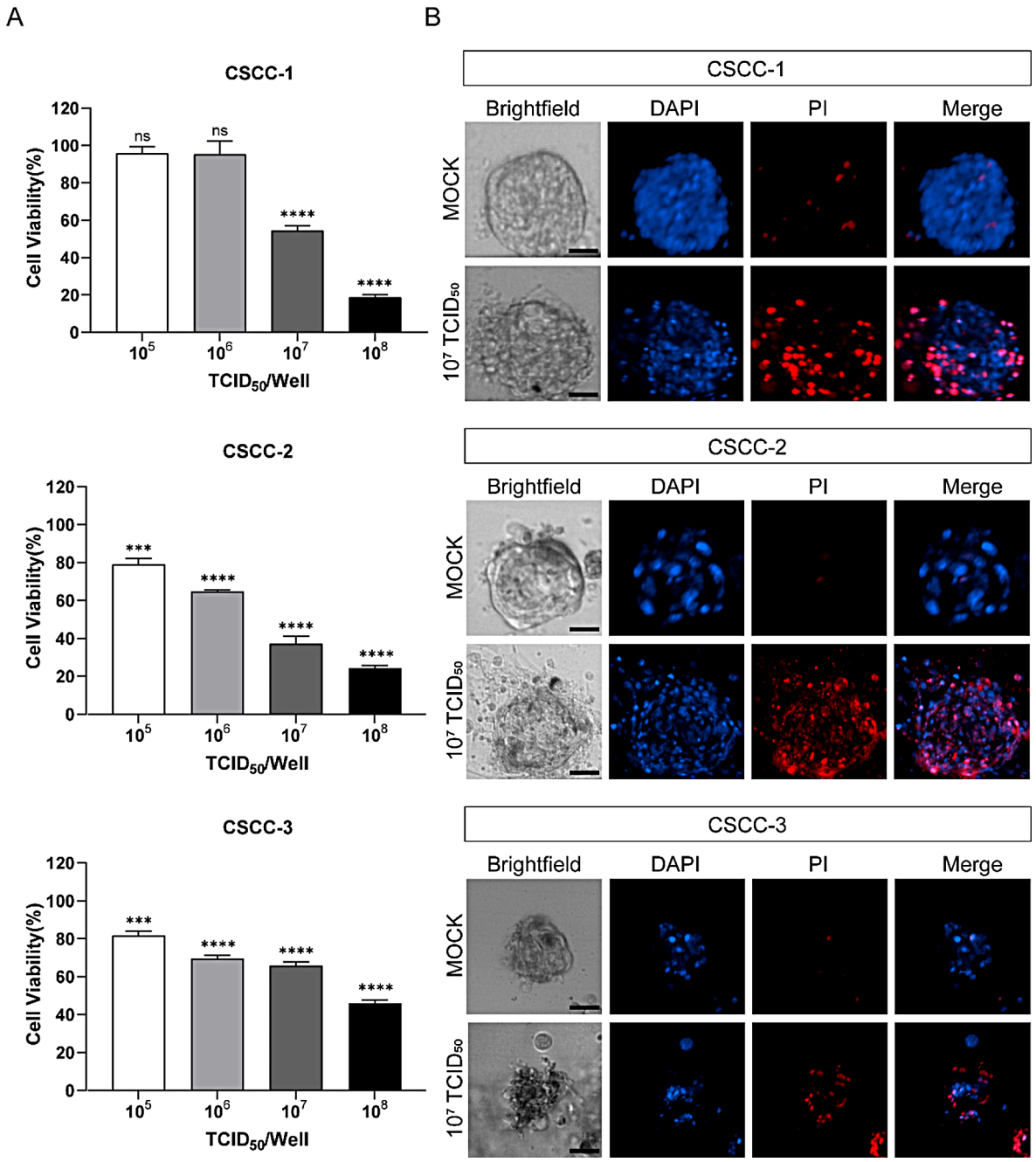

Fig. 4 Cytotoxic effects of CVB3/2035A on CSCC organoids. **(A)** CSCC organoids were exposed to 10-fold serial dilutions of CVB3/2035A and incubated at 37 ℃ for 72 h. Cell viability was evaluated using the Cell Titer-Glo 3D assay, with results presented as mean ± SEM ($n = 4$). Statistical analysis between CVB3/2035A-infected groups and the control group were assessed using One-way ANOVA followed by Tukey's test. ***$p < 0.001$; ****$p < 0.0001$; ns, not significant. **(B)** Representative images of CSCC organoids 72 h post-infection with 1×10^7 $TCID_{50}$/well CVB3/2035A. Dead cells were visualized with PI staining (red), while nuclei were counterstained with DAPI (blue). Scale bar, 50 µm

1×10^5 $TCID_{50}$/well, and virus titers were measured at 4, 12, 24, and 48 hpi. All organoid lines demonstrated an increase in viral titers across the four treatment doses (Fig. 5A). However, only at the higher doses of 1×10^7 or 1×10^8 $TCID_{50}$/well did peak titers show statistical significance compared to the virus titers at 4 hpi (within one virus replication cycle). The CSCC-1 and CSCC-2 organoid lines displayed faster viral growth kinetics than the CSCC-3 line. At the high dose of 1×10^8 TCID50/well, peak viral titers in the CSCC-1 and CSCC-2 organoid lines were achieved at 12 hpi, whereas the CSCC-3 organoid line peaked at 24 hpi (Fig. 5A). In addition, the peak viral titers in the CSCC-1 and CSCC-2 organoid lines were significantly higher than those in the CSCC-3

organoid line ($p=0.0260$ and $p=0.0296$, respectively; Fig. S6B). Notably, viral proliferation correlated with the level of cytotoxicity observed within the organoids.

Secondly, CSCC organoids treated with 1×10^7 $TCID_{50}$/well of CVB3/2035A were subjected to immunofluorescence staining for double-stranded RNA and the CVB3 VP1 protein at 72 hpi (Fig. 5B). Positive immunofluorescence staining confirmed the presence of viral nucleic acids and proteins within CSCC organoids, indicating viral spread within the organoids. Importantly, consistent colocalization between viral nucleic acids and the CVB3 VP1 protein was observed in consecutive sections spaced 5 μm apart. Together, these results demonstrate that CVB3/2035A effectively initiated productive infections in all CSCC organoid lines.

Synergistic antitumor effect of CVB3/2035A and paclitaxel in CSCC organoids

To evaluate the potential of enhancing conventional chemotherapy with CVB3/2035A-mediated oncolytic virotherapy for CSCC, patient-derived CSCC organoids were treated with PTX alone (2 μM), CVB3/2035A alone (1×10^7 $TCID_{50}$/well), or combinations of both (2 μM PTX plus 1×10^7, 1×10^6, or 1×10^5 $TCID_{50}$/well of CVB3/2035A). After 72 h post-treatment, PI staining was conducted to evaluate cytotoxic effects. The results showed that, compared to 2 μM PTX alone and 1×10^7

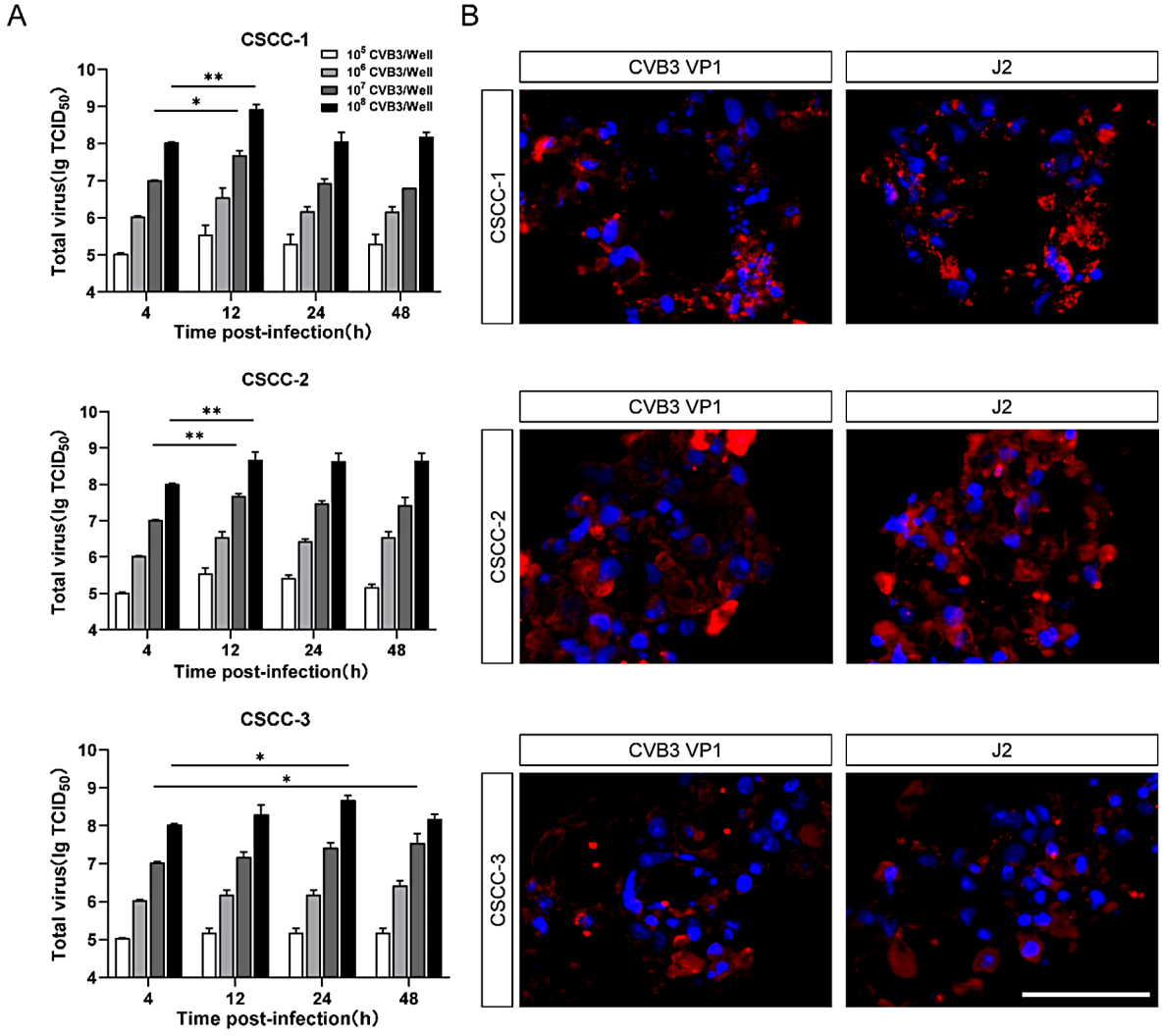

Fig. 5 Replication of CVB3/2035A in CSCC organoids. **(A)** Growth kinetics of CVB3/2035A in CSCC organoid lines. Following infection with 10-fold serial dilutions of CVB3/2035A (ranging from 1×10^8 to 1×10^5 TCID50/well), supernatant samples were collected at 4, 12, 24, and 48 hpi for viral titration by the $TCID_{50}$ assay. Statistical analysis of peak titers compared to the titers at 4 hpi was performed using two-way ANOVA. *$p<0.05$; **$p<0.01$. **(B)** Immunofluorescence analysis of CVB3/2035A infection in CSCC organoid lines. CSCC organoids, infected with 1×10^7 $TCID_{50}$/well of CVB3/2035A, were collected at 72 hpi and subjected to immunofluorescent staining for double-stranded RNA (J2) and the CVB3 VP1 protein (both in red). Nuclei were counterstained with DAPI (blue). Scale bar, 50 μm

$TCID_{50}$/well of CVB3/2035A alone, their combination resulted in a higher percentage of PI-positive cells in the CSCC organoids, suggesting an enhanced cytotoxic effect (Fig. 6A).

Next, to further quantify the cytotoxic effect among different groups, cell viability was assessed 72 h after treatment. In the PTX alone groups, cytotoxicity levels were 39.70±3.22%, 9.09±0.27%, and 11.69±0.77% for CSCC-1, CSCC-2, and CSCC-3 organoid lines, respectively. In the CVB3/2035A alone groups, 1×10^7 $TCID_{50}$/well of the virus induced cytotoxicity of 46.67±2.35%, 62.81±4.01%, and 34.17±1.87% in CSCC-1, CSCC-2, and CSCC-3 organoid lines, respectively. UV-inactivated CVB3/2035A (1×10^7 $TCID_{50}$/well) was used as a control and showed no cytotoxicity, indicating that oncolysis was induced by active viral replication of CVB3/2035A. In the combination groups, 2 μM PTX plus 1×10^7 $TCID_{50}$/well of CVB3/2035A induced cytotoxicity of 56.93±1.42%, 73.16±0.25%, and 48.20±2.97% in CSCC-1, CSCC-2, and CSCC-3 organoid lines, respectively. These results were significantly higher compared to the single-drug groups, suggesting a significant enhancement in cytotoxicity by the combination in all three organoid lines. Furthermore, this enhancement exhibited a dose-dependent response to the viral dosage (Fig. 6B).

To evaluate the influence of PTX on viral replication in the CSCC organoids, virus titers were compared between the group treated with 2 μM PTX plus 1×10^7 $TCID_{50}$/well of CVB3/2035A and the group treated with 1×10^7 $TCID_{50}$/well of CVB3/2035A alone at 4, 12, 24, and 48 hpi (Fig. 6C). The results showed that CVB3/2035A exhibited faster growth rates in the combination groups, especially during 0 to 12 hpi. Peak viral titers were observed at 12 hpi in all groups except the virus-alone group in CSCC-3, which reached peak titers at 24 hpi. Moreover, the combination groups consistently displayed higher peak viral titers than the virus-alone groups ($p=0.0474$, $p=0.0075$, and $p=0.0075$ in CSCC-1, CSCC-2, and CSCC-3, respectively). These results suggest that PTX significantly enhanced the viral replication of CVB3/2035A during oncolysis in the CSCC organoid lines.

Discussion

Oncolytic viruses are known for their unique ability to selectively target and destroy cancer cells while stimulating a systemic antitumor immune response. Among OVs, enteroviruses such as the recombinant poliovirus PVS-RIPO and the coxsackievirus A21-based CAVATAK have shown promising results in clinical trials, underscoring the potential of virotherapy [23, 24]. Recently, CVB3 strains targeting CAR-expressing cancer cells have demonstrated potent oncolytic activity and have been extensively studied [25–28]. Our previous research identified CVB3/2035A as an effective oncolytic strain against various cancer types, notably endometrial cancer [7]. In this study, we investigated the oncolytic effects of CVB3/2035A against CSCC, a prevalent malignancy among women worldwide. Current therapeutic approaches for CSCC often negatively impact women's quality of life, making oncolytic virotherapy a promising alternative strategy. Several OVs are under development for CSCC treatment [29].

To evaluate the efficacy of CVB3/2035A in CSCC, we first tested its oncolytic effects using cell lines and CDX models (Fig. 1). We then validated its oncolytic efficacy using patient-derived models. Specifically, we established ex vivo tumor tissue cultures from a limited number of CSCC patient tissues for preliminary verification and focused on evaluating the oncolytic activity of CVB3/2035A in high-throughput CSCC organoid models. Our results revealed dose-dependent cytotoxicity and significant viral replication within the CSCC organoids (Figs. 4A and 5). The increased viral titers and the presence of viral RNA and proteins indicated that the cytotoxic effect on organoid cells was closely tied to viral replication. These data suggest that CVB3/2035A possesses significant oncolytic potential against CSCC.

Currently, various organoid models have been employed for drug evaluation, demonstrating consistent responses between patients and cancer organoids [12, 13, 30]. CSCC organoids preserve the original features of tumors, making them valuable models for precision medicine [2, 12]. In our study, the established CSCC organoids closely resembled the original tumors in terms of tumor-associated biomarkers (Fig. 3D-E, Fig. S5). Specifically, CSCC organoids expressed the major receptor CAR for CVB3 binding and uptake. CAR expression levels or CAR-positive cell proportions correlated positively with their sensitivity to CVB3/2035A infection and lysis (Figs. 3E, 4 and 5 and Fig. S6), consistent with results from cell lines and ex vivo tissue cultures (Figs. 1 and 2, Fig. S1 and Fig. S3). CSCC organoids provide a clinically relevant model to evaluate the direct oncolytic effects of CVB3/2035A against CSCC cells in vitro. However, the lack of stromal components in patient-derived organoids (PDOs) is a limitation, given the important role of the tumor microenvironment in anticancer therapies. Future studies should focus on 3D co-cultures that include PDOs, fibroblasts, and/or immune cells to better model tumor complexity for evaluating virotherapy responses [10, 31]. In addition, PDX models that maintain tumor architecture and relative proportions of cancer and stromal cells, along with humanized mouse models featuring a reconstituted human immune system, can be utilized to evaluate the influence of tumor microenvironment and immune system on the oncolytic effect in vivo [9, 32].

PTX is a common chemotherapy drug for cervical cancer. Our study found that the combination of

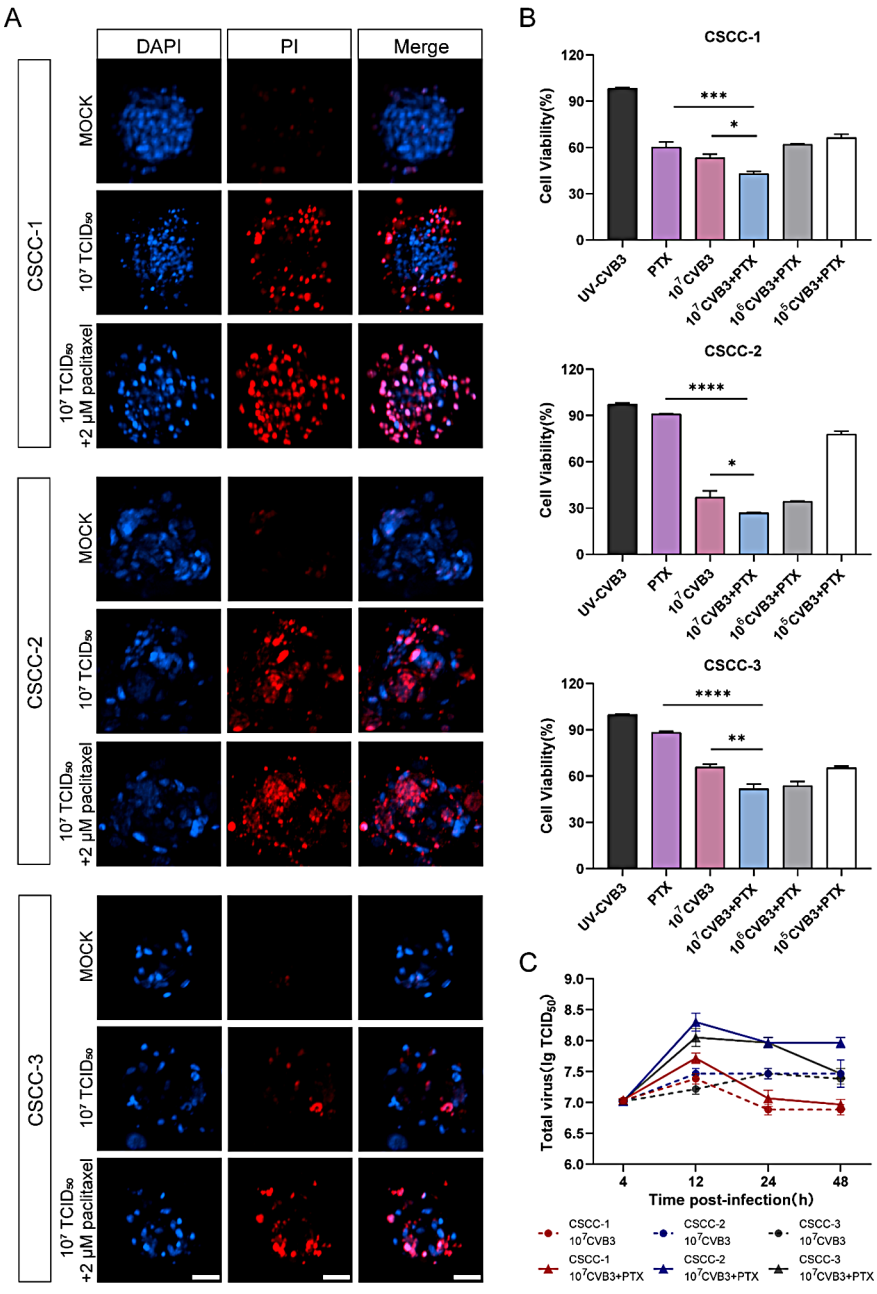

Fig. 6 Combined treatment of CVB3/2035A and paclitaxel for CSCC organoids. **(A)** Representative images of CSCC organoids 72 h post-infection with 1×10^7 $TCID_{50}$/well CVB3/2035A, with or without 2 μM PTX. Dead cells were visualized with PI staining (red), while nuclei were counterstained with DAPI (blue). Scale bar, 50 μm. **(B)** CSCC organoid lines were treated with 2 μM PTX, 1×10^7 $TCID_{50}$/well CVB3/2035A, or 2 μM PTX plus 10-fold diluted CVB3/2035A (ranging from 1×10^7 to 1×10^5 $TCID_{50}$/well). Cell viability was evaluated using the Cell Titer-Glo 3D assay, with results presented as mean ± SEM. Statistical analysis was performed using one-way ANOVA followed by Tukey's test. *$p < 0.05$; **$p < 0.01$; ***$p < 0.001$; ****$p < 0.0001$. **(C)** Comparison of viral growth kinetics between groups treated with 2 μM PTX plus 1×10^7 $TCID_{50}$/well CVB3/2035A and those treated with 1×10^7 $TCID_{50}$/well CVB3/2035A alone. Data are represented as mean ± SEM, statistical analysis for virus peak titer was performed using Student's *t*-test

CVB3/2035A and PTX significantly improved efficacy compared to either treatment alone, without compromising the virus's safety profile (Figs. 1D and 6, Fig. S1C and Fig. S2). Moreover, the combination treatment significantly increased the cytotoxic effect on CSCC organoids (Fig. 6B), likely due to higher production of the CVB3/2035A virus (Fig. 6C). Previous studies on the oncolytic herpesvirus T-VEC and other oncolytic viruses have also shown the synergistic potential of combining PTX with oncolytic viruses. This synergistic effect may be related to microtubule stabilization, mitotic arrest, apoptosis, and interferon secretion [17, 22, 33, 34], as

well as alterations in the tumor microenvironment such as enhanced infiltration of lymphoid and myeloid cells [35, 36]. Together, these results support the combination of CVB3/2035A and PTX for CSCC therapy.

CVB3/2035A, an RNA virus, replicates in the cytoplasm through negative-sense RNA intermediates, thereby avoiding the genotoxicity associated with viral genome integration into host DNA [37]. Although certain CVB3 strains can cause severe diseases [25, 38], naturally occurring non-pathogenic strains, such as CVB3/026 [39], CVB3/GA27 [40], and CVB3/PD28 [28], exhibit evolutionary stability and potential for oncolytic virus therapy. Consistent with our previous study [7], this study found no mortality or weight loss in mice treated with CVB3/2035A (Fig. S1B-C), and no pathological changes were observed in major organs, including the heart, liver, spleen, lung, kidney, brain, and pancreas (Fig. S2). Moreover, CVB3/2035A demonstrated significant cytotoxic effects in ex vivo cultured tissue slices derived from endometrial cancer and CSCC patients while sparing normal endometrial and cervical tissues. This tumor selectivity appeared to be related to markedly higher CAR expression levels in tumor tissues compared to normal tissues (Fig. S3). These data suggest that CVB3/2035A may be a non-pathogenic or low-virulence strain. To further enhance the safety and tumor selectivity of CVB3/2035A, future studies could incorporate target sequences of microRNAs (miRs) highly expressed in normal tissues but downregulated in cancer tissues (e.g., miR-1, miR-34, miR-143, miR-145, miR-216, and miR-217) into the CVB3/2035A viral genome. This microRNA-mediated regulation of virus replication has been shown to effectively detarget the virus from healthy tissues without compromising its oncolytic activity in cancer [38, 41–43].

Conclusions

In summary, CVB3/2035A exhibits potent oncolytic activity in CSCC cell lines, CDXs, patient-derived tissues, and organoids. In addition, CVB3/2035A demonstrates synergistic effectiveness with PTX for CSCC treatment. Future studies should aim to elucidate the mechanisms underlying the oncolytic effects of CVB3/2035A and its synergistic interactions with PTX in CSCC, improve the safety and efficacy of CVB3/2035A through reverse genetics, and explore the potential of combining CVB3/2035A with other therapeutic drugs or methods for CSCC treatment.

Abbreviations

CSCC	Cervical squamous cell carcinoma
OV	Oncolytic virus
CVB3	Coxsackievirus B3
CVB3/Nancy	Coxsackievirus B3 Nancy strain
CVB3/2035A	Coxsackievirus B3 2035 A strain
CAR	Coxsackievirus and adenovirus receptor
CDX	Cell line-derived xenograft
PDX	Patient-derived tumor xenograft
PTX	Paclitaxel
FITC	Fluorescein isothiocyanate
i.t.	intratumoral
i.v.	intravenous
i.p.	intraperitoneal
Mins	Minutes
IHC	Immunohistochemistry
BME	Basement membrane extract
PI	Propidium iodide
hpi	hours post-infection
PDOs	Patient-derived organoids
miRs	microRNAs

Supplementary Information

The online version contains supplementary material available at https://doi.org/10.1186/s12985-024-02502-y.

Supplementary Material 1

Acknowledgements

Not applicable.

Author contributions

YZL, NYL, and CLY designed the experiments. YZL, NYL, CLY, HYT, CJF, KY and HZ carried out the experiments. YZL, NYL, NSX, WW, XMH and TC analyzed the data. YZL, NYL, WW, XMH and TC wrote and edited the paper. All authors read and approved the final manuscript.

Funding

This research was supported by the Natural Science Foundation of Fujian Province of China (No.2022J011352) and the National Natural Science Foundation of China (No. 82272310, 82171833 and 82072282).

Data availability

No datasets were generated or analysed during the current study.

Declarations

Ethics approval and consent to participate

Human CSCC samples were collected from patients at Zhongshan Hospital of Xiamen University during surgical resection procedures. Informed consent for this study was obtained from each patient. This study was approved by the Institutional Review Board of the hospital and the Research Ethics Committee of Xiamen University. Experiments were carried out in strict accordance with the guidelines and regulations of Xiamen University.

Consent for publication

Not applicable.

Competing interests

The authors declare no competing interests.

Author details

[1]Department of Obstetrics and Gynecology, Zhongshan Hospital, Xiamen University, Xiamen 361004, China
[2]State Key Laboratory of Vaccines for Infectious Diseases, Xiang An Biomedicine Laboratory, School of Life Sciences, School of Public Health, Xiamen University, Xiamen 361102, China
[3]National Institute of Diagnostics and Vaccine Development in Infectious Diseases, National Innovation Platform for Industry-Education Integration in Vaccine Research, Xiamen University, Xiamen 361102, China

Received: 14 May 2024 / Accepted: 12 September 2024
Published online: 05 October 2024

References

1. Sung H, Ferlay J, Siegel RL, Laversanne M, Soerjomataram I, Jemal A, et al. Global Cancer statistics 2020: GLOBOCAN estimates of incidence and Mortality Worldwide for 36 cancers in 185 countries. CA Cancer J Clin. 2021;71(3):209–49.
2. Lõhmussaar K, Oka R, Espejo Valle-Inclan J, Smits MHH, Wardak H, Korving J, et al. Patient-derived organoids model cervical tissue dynamics and viral oncogenesis in cervical cancer. Cell Stem Cell. 2021;28(8):1380–e966.
3. Cohen PA, Jhingran A, Oaknin A, Denny L. Cervical cancer. Lancet. 2019;393(10167):169–82.
4. Lin D, Shen Y, Liang T. Oncolytic virotherapy: basic principles, recent advances and future directions. Signal Transduct Target Ther. 2023;8(1):156.
5. Shalhout SZ, Miller DM, Emerick KS, Kaufman HL. Therapy with oncolytic viruses: progress and challenges. Nat Rev Clin Oncol. 2023;20(3):160–77.
6. Geisler A, Hazini A, Heimann L, Kurreck J, Fechner H. Coxsackievirus B3-Its potential as an Oncolytic Virus. Viruses. 2021;13(5).
7. Lin Y, Wang W, Wan J, Yang Y, Fu W, Pan D, et al. Oncolytic activity of a coxsackievirus B3 strain in human endometrial cancer cell lines. Virol J. 2018;15(1):65.
8. Reeh M, Bockhorn M, Görgens D, Vieth M, Hoffmann T, Simon R, et al. Presence of the Coxsackievirus and Adenovirus receptor (CAR) in human neoplasms: a multitumour array analysis. Br J Cancer. 2013;109(7):1848–58.
9. Liu L, Wu M, Huang A, Gao C, Yang Y, Liu H et al. Establishment of a high-fidelity patient-derived xenograft model for cervical cancer enables the evaluation of patient's response to conventional and novel therapies. J Translational Med. 2023;21(1).
10. Bleijs M, van de Wetering M, Clevers H, Drost J. Xenograft and organoid model systems in cancer research. EMBO J. 2019;38(15).
11. Hoffmann C, Bachran C, Stanke J, Elezkurtaj S, Kaufmann AM, Fuchs H, et al. Creation and characterization of a xenograft model for human cervical cancer. Gynecol Oncol. 2010;118(1):76–80.
12. Veninga V, Voest EE. Tumor organoids: opportunities and challenges to guide precision medicine. Cancer Cell. 2021;39(9):1190–201.
13. Vlachogiannis G, Hedayat S, Vatsiou A, Jamin Y, Fernandez-Mateos J, Khan K et al. Patient-derived organoids model treatment response of metastatic gastrointestinal cancers. Science. 2018.
14. Sachs N, de Ligt J, Kopper O, Gogola E, Bounova G, Weeber F et al. A living biobank of breast Cancer Organoids captures Disease Heterogeneity. Cell. 2018;172(1–2):373 – 86 e10.
15. Hill SJ, Decker B, Roberts EA, Horowitz NS, Muto MG, Worley MJ Jr., et al. Prediction of DNA repair inhibitor response in short-term patient-derived ovarian Cancer Organoids. Cancer Discov. 2018;8(11):1404–21.
16. Puca L, Bareja R, Prandi D, Shaw R, Benelli M, Karthaus WR, et al. Patient derived organoids to model rare prostate cancer phenotypes. Nat Commun. 2018;9(1):2404.
17. Ingemarsdotter CK, Baird SK, Connell CM, Oberg D, Hallden G, McNeish IA. Low-dose paclitaxel synergizes with oncolytic adenoviruses via mitotic slippage and apoptosis in ovarian cancer. Oncogene. 2010;29(45):6051–63.
18. Koikawa K, Kibe S, Suizu F, Sekino N, Kim N, Manz TD, et al. Targeting Pin1 renders pancreatic cancer eradicable by synergizing with immunochemotherapy. Cell. 2021;184(18):4753–e7127.
19. Jun E, Park Y, Lee W, Kwon J, Lee S, Kim MB et al. The identification of candidate effective combination regimens for pancreatic cancer using the histoculture drug response assay. Sci Rep. 2020;10(1).
20. Kopper O, de Witte CJ, Lohmussaar K, Valle-Inclan JE, Hami N, Kester L, et al. An organoid platform for ovarian cancer captures intra- and interpatient heterogeneity. Nat Med. 2019;25(5):838–49.
21. Li Z, Xu H, Gong Y, Chen W, Zhan Y, Yu L et al. Patient-derived Upper Tract Urothelial Carcinoma Organoids as a platform for drug screening. Adv Sci. 2021;9(4).
22. Bourgeois-Daigneault MC, St-Germain LE, Roy DG, Pelin A, Aitken AS, Arulanandam R, et al. Combination of Paclitaxel and MG1 oncolytic virus as a successful strategy for breast cancer treatment. Breast Cancer Res. 2016;18(1):83.
23. Annels NE, Arif M, Simpson GR, Denyer M, Moller-Levet C, Mansfield D, et al. Oncolytic immunotherapy for bladder Cancer using Coxsackie A21 Virus. Mol Ther Oncolytics. 2018;9:1–12.
24. Annels NE, Mansfield D, Arif M, Ballesteros-Merino C, Simpson GR, Denyer M, et al. Phase I trial of an ICAM-1-Targeted immunotherapeutic-Coxsackievirus A21 (CVA21) as an Oncolytic Agent Against non muscle-invasive bladder Cancer. Clin Cancer Res. 2019;25(19):5818–31.
25. Miyamoto S, Inoue H, Nakamura T, Yamada M, Sakamoto C, Urata Y, et al. Coxsackievirus B3 is an oncolytic virus with immunostimulatory properties that is active against lung adenocarcinoma. Cancer Res. 2012;72(10):2609–21.
26. Deng H, Liu H, de Silva T, Xue Y, Mohamud Y, Ng CS, et al. Coxsackievirus Type B3 is a potent oncolytic virus against KRAS-Mutant Lung Adenocarcinoma. Mol Therapy - Oncolytics. 2019;14:266–78.
27. Bahreyni A, Mohamud Y, Ashraf Nouhegar S, Zhang J, Luo H. Synergistic viro-chemoimmunotherapy in breast Cancer enabled by Bioengineered Immunostimulatory exosomes and Dual-targeted Coxsackievirus B3. ACS Nano. 2024;18(5):4241–55.
28. Hazini A, Pryshliak M, Bruckner V, Klingel K, Sauter M, Pinkert S, et al. Heparan Sulfate binding Coxsackievirus B3 strain PD: a Novel Avirulent Oncolytic Agent Against Human Colorectal Carcinoma. Hum Gene Ther. 2018;29(11):1301–14.
29. Kalafati E, Drakopoulou E, Anagnou NP, Pappa KI. Developing oncolytic viruses for the treatment of Cervical Cancer. Cells. 2023;12(14).
30. Yan HHN, Chan AS, Lai FP, Leung SY. Organoid cultures for cancer modeling. Cell Stem Cell. 2023;30(7):917–37.
31. Raimondi G, Mato-Berciano A, Pascual-Sabater S, Rovira-Rigau M, Cuatrecasas M, Fondevila C, et al. Patient-derived pancreatic tumour organoids identify therapeutic responses to oncolytic adenoviruses. EBioMedicine. 2020;56:102786.
32. Yoshida GJ. Applications of patient-derived tumor xenograft models and tumor organoids. J Hematol Oncol. 2020;13(1).
33. Soliman H, Hogue D, Han H, Mooney B, Costa R, Lee MC, et al. Oncolytic T-VEC virotherapy plus neoadjuvant chemotherapy in nonmetastatic triple-negative breast cancer: a phase 2 trial. Nat Med. 2023;29(2):450–7.
34. Lin SF, Gao SP, Price DL, Li S, Chou TC, Singh P, et al. Synergy of a herpes oncolytic virus and paclitaxel for anaplastic thyroid cancer. Clin Cancer Res. 2008;14(5):1519–28.
35. Deng X, Shen Y, Yi M, Zhang C, Zhao B, Zhong G et al. Combination of novel oncolytic herpesvirus with paclitaxel as an efficient strategy for breast cancer therapy. J Med Virol. 2023;95(5).
36. Shinoda S, Sharma NS, Nakamura N, Inoko K, Sato-Dahlman M, Murugan P, et al. Interferon-expressing oncolytic adenovirus + chemoradiation inhibited pancreatic cancer growth in a hamster model. Cancer Sci. 2023;114(9):3759–69.
37. Liu H, Luo H. Development of Group B Coxsackievirus as an Oncolytic Virus: opportunities and challenges. Viruses. 2021;13(6).
38. Jia Y, Miyamoto S, Soda Y, Takishima Y, Sagara M, Liao J, et al. Extremely low Organ toxicity and strong antitumor activity of mir-34-Regulated Oncolytic Coxsackievirus B3. Mol Ther Oncolytics. 2019;12:246–58.
39. Gauntt CJ, Trousdale MD, LaBadie DR, Paque RE, Nealon T. Properties of coxsackievirus B3 variants which are amyocarditic or myocarditic for mice. J Med Virol. 1979;3(3):207–20.
40. Lee CK, Kono K, Haas E, Kim KS, Drescher KM, Chapman NM, et al. Characterization of an infectious cDNA copy of the genome of a naturally occurring, avirulent coxsackievirus B3 clinical isolate. J Gen Virol. 2005;86(Pt 1):197–210.
41. Liu H, Xue YC, Deng H, Mohamud Y, Ng CS, Chu A, et al. MicroRNA modification of Coxsackievirus B3 decreases its toxicity, while retaining Oncolytic Potency against Lung Cancer. Mol Ther Oncolytics. 2020;16:207–18.
42. Bahreyni A, Liu H, Mohamud Y, Xue YC, Zhang J, Luo H. A new miRNA-Modified coxsackievirus B3 inhibits triple negative breast cancer growth with improved safety profile in immunocompetent mice. Cancer Lett. 2022;548:215849.
43. Sagara M, Miyamoto S, Itoh S, Soda Y, Tani K. Development of New Oncolytic Virotherapy targeting breast Cancer using Coxsackievirus B3. Anticancer Res. 2021;41(1):81–9.

Publisher's note